Evaluating the pressure-leakage behaviour of leaks in water pipes

Short title: Evaluating the pressure-leakage behaviour of leaks in water pipes

J. E. van Zyl[a,*] *and R. Malde*[b]

[a]*Department of Civil Engineering, University of Cape Town, South Africa*

[b]*Weld-Con Ltd., Mombasa, Kenya*

*Corresponding author. E-mail address: kobus.vanzyl@uct.ac.za.

ABSTRACT

Much progress has been made over the last decade in understanding the behaviour of flow through leak openings with changes in water mains pressure. In particular it has been established that variations in leak areas with pressure is the main factor responsible for the range of leakage exponents observed in practice, and several numerical and experimental studies have investigated this behaviour. This paper provides an overview of the advances in leakage modelling over the last decade and then presents the results of a new experimental study of various leak types (round holes and longitudinal, spiral and circumferential cracks) in different pipe materials (uPVC, mPVC, HDPE and steel). The experimental results are evaluated in light of the latest theoretical advances and recommendations are made for further experimental studies.

[Water losses; leakage; pressure; FAVAD; N1]

INTRODUCTION

The International Water Association (IWA) has been at the forefront of water loss management for several decades. Their efforts were formalised in 1995 with the formation of the Water Loss Task Force, which has made extensive contributions to the field, including the internationally used IWA Water Balance, Infrastructure Leakage Index (ILI) and several other benchmarks and guidelines (Lambert 2015).

One of the important activities of the IWA Water Loss Task Force (now the Water Loss Specialist Group) has been to investigate why leak flow rates are often significantly more sensitive to pressure than predicted by the orifice equation (Lambert 1997, 2000; Lambert *et al.* 2013).

Hydraulically, pipe leaks are orifices and thus can reasonably be expected to comply with the orifice equation, which is derived from the principle of conservation of energy. According to the orifice equation, the flow rate Q through a leak should be proportional to the square root of the pressure head differential h over the leak opening as described by:

$$Q = C_d A\sqrt{2gh} \tag{1}$$

where C_d is the discharge coefficient, A leak area and g acceleration due to gravity.

However, since the results of numerous international field studies have shown that the orifice equation often does not fit the measured pressure-leakage response, a power equation (known as the N1 power equation) has been adopted by the IWA and has become widely used (Gebhardt 1975; Ogura 1979; Hiki 1981; Lambert 2000; Farley & Trow 2003; Al-Ghamdi 2011):

$$Q_L = Ch^{N1} \tag{2}$$

where Q_L is the power equation leakage rate, C is the leakage coefficient and N1 the leakage exponent. It should be noted that making the exponent of the leakage equation a variable severs it from its fluid mechanics foundations and turns it into a purely empirical equation. Thus the power equation approach is not standard practice in orifice hydraulic theory (Idelchick 1994; Franchini *et al.* 2014).

While the value of N1 should be 0.5 to comply with the orifice equation, in field studies it has been found to range between 0.36 and 2.95 (see Schwaller *et al.* (2014) for a summary of the ranges for N1 found in different countries).

It is important to understand the causes of the observed high leakage exponent values as this may allow engineers to better predict the response of systems to changes in pressure, and ultimately improve the management of leakage. Van Zyl & Clayton (2007) proposed a number of potential causes of the observed range of N1 values, including leak hydraulics, soil hydraulics and variations in leak area with pressure. Other factors have also been shown to play a role, including errors in field test assessment of average pressure and leakage estimates, the spatial distribution of leaks (Schwaller & Van Zyl 2014; Schwaller *et al.* 2015), soils surrounding the pipe (Walski *et al.* 2006; Van Zyl *et al.* 2013) and changes in axial momentum (Ferrante *et al.* 2013). It is now widely accepted that changes in leak area are the most important causative factor of the observed behaviour.

In 2007, Greyvenstein & Van Zyl published the results of an exploratory experimental study in the Journal of Water Supply: Research and Technology – AQUA, showing that the leakage exponents measured in the field are not unrealistic, and can be reproduced in the laboratory. They found leakage exponents between 0.41 and 2.30 and agreed that variation in leak area is the most likely cause for the deviation from the orifice equation.

Significant progress on understanding the behaviour of leaks areas in pipes has been made in the last decade. Thus the aims of this paper are two-fold: to provide a review and synthesis of developments in understanding leakage behaviour over the last decade and to present the results of a recent experimental study in the light of these findings. It is hoped that the proposed experimental method and data analysis will provide a uniform basis for the further experimental work required to establish the characteristics of the various leak types in different pipe materials and sections, including service connections and leaks at joints and fittings.

The next section provides an overview of the current understanding of leak area behaviour and its implications for leakage modelling and management. This is followed by the description of a proposed standard experimental procedure and data analysis of different leak types (round

holes and longitudinal, spiral and circumferential cracks) in different pipe materials (unplasticised PVC, modified PVC, HDPE and steel).

LEAK AREA VARIATION AND ITS IMPLICATIONS FOR LEAKAGE MODELLING

Pressure and pipe wall stresses

Pressure in a water pipe causes stresses to develop in the pipe walls, resulting in material strain and subsequently changes in the areas of leak openings in pipes. It is possible to derive theoretical equations for the circumferential and longitudinal stresses in a closed cylindrical container resulting from water pressure (for instance, see Cassa *et al.* 2010). These equations show that both circumferential and longitudinal stresses are linear functions of the pressure, but that the circumferential stresses are double the size of the longitudinal stresses.

However, unlike pressure vessels, pipes are not closed at their ends and are generally supported by thrust blocks at bends and junctions that transfer the longitudinal forces to the soil. Thus it is the circumferential rather than longitudinal pipe wall stresses that will vary as a result of changes in pressure.

It should be noted that several external factors, such as the weight of soil, external loads, soil movements and thermal expansions also influence the pipe wall stresses. However, unlike the circumferential stresses induced by fluid pressure, these stresses are independent of water pressure and thus are likely to have a constant impact on leak area variations.

Linearity of the pressure-area relationship

The mechanisms through which pipe material can deform in response to changes in pressure are elastic, viscoelastic and plastic deformation and fracture.

Over the last decade, several experimental and modelling studies have been carried out under elastic deformation conditions on a large range of pipe materials, section properties, leak types and loading conditions. These studies concluded that all leak areas vary as a linear function of pressure (Buckley 2007; Cassa & Van Zyl 2013; Van Zyl & Cassa 2014).

Plastics such as PVC and PE are viscoelastic materials, which means that they display both elastic and viscous deformation behaviour. Several researchers have investigated the resultant time-dependent response of leak areas to changes in pressure (Ferrante *et al.* 2011, 2013; Ferrante 2012; Massari *et al.* 2012; De Marchis *et al.* 2016; Fox *et al.* 2016a, 2016b). Ssozi *et al*. (2016) showed that at any given time after loading, plastic pipes also have a linear pressure-area relationship, but that the slope of the relationship increases with time until it stabilises at the relaxation time of the material.

Unlike the elastic and viscoelastic cases, leak areas in pipes undergoing plastic (permanent) deformation or fracture cannot be assumed to have linear pressure-area relationships. However, both these processes are non-reversible and can thus only continue for a limited time before they will either stabilise (i.e. become elastic or viscoelastic) or result in catastrophic fracture

(Buckley 2007). In addition, they can only occur when the water pressure is increased (i.e. pipe wall stresses are increased) and not when the pressure is decreased. Since zonal pressure management virtually always involves lowering of pressures, the effects of plastic deformation and fracture may be ignored in analysing pressure management zone data.

The observed relationship between pressure and leak area can now be described with the following function:

$$A = A_0 + mh \tag{3}$$

where A_0 is the initial area (the area of the leak opening at zero head differential) and m the head-area slope.

The linearity of the pressure-leakage relationship means that it is only necessary to know a leak opening's initial area and head-area slope to fully characterise its area and thus its hydraulic behaviour using Equation (1). The following points summarise the main findings on the head-area slope of pipe leaks (Greyvenstein & van Zyl 2007; Cassa *et al.* 2010; Cassa & van Zyl 2013; Van Zyl & Cassa 2014):

- The areas of round holes in all materials are stable and vary very little with pressure. In practice this means that their head-area slopes may be assumed to be zero.
- The head-area slopes of all types of leaks in steel pipes are very small and may also be assumed to be zero. However, corrosion failures in metal pipes have not been studied in detail and further work is required to determine whether reduced wall thicknesses due to corrosion will have a significant effect on the head-area slope.
- The head-area slopes of circumferential cracks are generally small and often negative, meaning that the crack area reduces with increasing pressure (a result of the circumferential stresses elongating the crack, pulling it closed due to the Poisson's ratio effect).
- Longitudinal cracks have the largest head-area slopes of all leak types. Cassa & Van Zyl (2013) found that the crack width and Poisson's ratio of the pipe material had a negligible effect on the head-area slope. They proposed an equation for predicting the head-area slope of longitudinal cracks as a function of the pipe diameter d, crack length L_c, elasticity modulus of the pipe material E and pipe wall thickness t (ρ is the density of water and g acceleration due to gravity):

$$m = \frac{2.93157 d^{0.3379} L_c^{4.80} 10^{0.5997(\log L_c)^2} \rho g}{E t^{1.746}} \tag{4}$$

Van Zyl & Cassa (2014) showed that this equation provides good results based on data from several different laboratory studies.

Implications for leak hydraulics

To understand the impact of the observed linear head-area relationship on leak hydraulics, Equation (3) is replaced in Equation (1) to obtain:

$$Q = C_d\sqrt{2g}(A_0 h^{0.5} + mh^{1.5}) \quad (5)$$

The form of this equation was earlier proposed by Ledochowski (1956) and particularly May (1994) whose paper became highly influential as the FAVAD (Fixed and Variable Area Discharges) equation.

The first term of Equation (5) is the orifice equation and describes the flow through a fixed initial area of the leak. The second term in the equation describes the flow through the expanded area of the leak.

It should be noted that while the discharge coefficient C_d is an unknown in Equation (5), it can be eliminated by combining it with the initial area and head-area slope. In this arrangement, A' is called the effective area ($A' = C_d A$), A'_0 the effective initial area ($A'_0 = C_d A_0$) and m' the effective head-area slope ($m' = C_d m$). Equations (3) and (5) now become:

$$A' = A'_0 + m'h \quad (6)$$

and

$$Q = \sqrt{2g}(A'_0 h^{0.5} + m'h^{1.5}) \quad (7)$$

Van Zyl & Cassa (2014) proposed a dimensionless leakage number L_N defined as the ratio of the flow through the expanded to the initial leak areas, and this is given by:

$$L_N = \frac{mh}{A_0} \quad (8)$$

They then showed that there is a direct relationship between N1 and the leakage number described by the equation:

$$N1 = \frac{1.5L_N + 0.5}{L_N + 1} \quad (9)$$

While Equation (5) or (7) seems to predict a leakage exponent between 0.5 and 1.5, it can be seen from Equation (9) that the leakage exponent can adopt a wider range. In particular, the leakage exponent will approach infinity when the leakage number approaches minus one.

The implications for leakage modelling can be summarised as follows (Van Zyl & Cassa 2014; Van Zyl *et al.*, in press):

- The N1 power equation is an empirical equation not based on fundamental fluid mechanics principles. It can provide reliable results when used within its calibration pressure range, but may result in significant errors if used to extrapolate beyond this range.
- The leakage exponent of a system (with a given set of leaks) is not constant, but varies with system pressure. Higher pressures in the same system will result in higher N1 values, while lower pressures will result in lower N1 values.

- While the head-area slope is not affected by the width of a crack, the leakage number (Equation (8)) is significantly affected due to the change in the initial area. From Equation (9) it can now be shown that the same crack will have substantially higher leakage exponents at smaller crack widths. The implication of this observation is that the leakage exponents determined in laboratory tests, where a slit is normally machined into a pipe, will tend to underestimate the leakage exponent of the same crack length that forms in the field without removal of pipe material (and thus with a smaller width).
- Finally, it can be shown from Equations (6)–(9) that leak openings with negligibly small head area slopes (i.e. fixed leak openings) will result in N1 = 0.5 and leak openings with initial areas close to zero (such as cracks closing under zero pressure conditions) will result in N1 = 1.5.

Implications for DMA leakage modelling

Leakage in water distribution systems is normally assessed at DMA level through minimum night flow and water balance analyses. While larger leaks can mostly be detected and repaired, little is known about the number and distribution of smaller background leaks.

The behaviour of systems with many leaks adhering to the power leakage equation was studied by Ferrante *et al*. (2014), who found that the DMA leakage exponent is larger than the mean individual leakage exponent due to the spatial variability of leaks. Schwaller & van Zyl (2014) found that individual leaks adhering to the FAVAD equation can result in a wide range of DMA leakage exponents, similar to that observed in practice.

The linearity of the leak area-pressure relationship has important implications for the understanding of DMA leakage behaviour. In particular it means that the total DMA leakage, which is the sum of the individual leak behaviours, will also be a linear function of average zone pressure and that Equations (3) and (5)–(8) can thus be applied to DMAs with many leaks.

In practice this means that if the DMA leakage at the time of steady minimum night flow is known at two different Average Zone Night Pressures (AZNPs), which are currently used to determine N1 using Equation (2), the same data may be used in Equation (7) to estimate the sum of effective initial areas and head area slopes for all the leaks – both detectable and non-detectable – in the DMA.

The resulting DMA initial area provides an estimate for the total leak area under zero pressure conditions and the DMA effective head-area slope can be used in combination with the known values for different leak types to estimate the dominant leak type in the DMA. In addition the N1 for the DMA can be estimated at different pressures from its initial area and head-area slope using Equations (8) and (9).

Schwaller *et al* (2015) used a spreadsheet model with stochastic leak distributions to confirm that the initial area and head-area slope of a DMA provide good estimates of the sum of the initial areas and head-area slopes of individual leaks in the system respectively. Unrealistic values of the system leakage parameters may be used to diagnose potential problems, such as

measurement errors or leaking boundary valves (this is already the case in the expert software PresCalcs (Lambert 2016)).

Finally, Kabaasha *et al* (2016) incorporated the FAVAD approach into hydraulic network models and showed that significant errors in the leakage demand at nodes can be made when the current power equation approach is used.

The next section of the paper reports on the results of an experimental study of the pressure-leakage behaviour of pipe leaks, and analyses these results in light of the theory discussed in this section.

EXPERIMENTAL STUDY

Introduction

An experimental study was conducted to investigate the behaviour of various types of leaks (round holes and longitudinal, spiral and circumferential cracks) in 100 mm nominal diameter pipes of different materials predominantly used for distribution mains. The pipe materials that were included in the study were uPVC (unplasticised polyvinylchloride), mPVC (modified polyvinylchloride), HDPE (high density polyethylene) and steel. mPVC is a pipe material designed to have additional ductility and more stable long-term characteristics than uPVC (DPI 2010).

The properties and dimensions of the leaks and pipes used in this study are summarised in Table 1. The elasticity modulus of the materials were not measured, but estimated from literature. All cracks had a width of 1 mm.

Table 1 | Properties and dimensions of the leaks and pipes investigated in this study

				Main dimensions of leaks tested (mm)			
					Cracks		
Pipe material	**Internal diameter (mm)**	**Wall thickness (mm)**	**Elasticity modulus E (MPa)**	**Round holes**	**Longi-tudinal**	**Spiral**	**Circum-ferential**
uPVC	105.5	4.54	3	12	50, 100	50, 100	50, 100
mPVC	106.6	3.44	3	12	50	50	50
HDPE	103.6	6.38	1	12	73, 100	50, 78	54, 80
Steel	105.1	4.92	203	12	50, 100	50, 105	53

Experimental setup and procedure

The main component of the experimental setup is shown in Figure 1 and consisted of two removable end sections fitted to a sample pipe section with a failure using flexible couplings.

a)

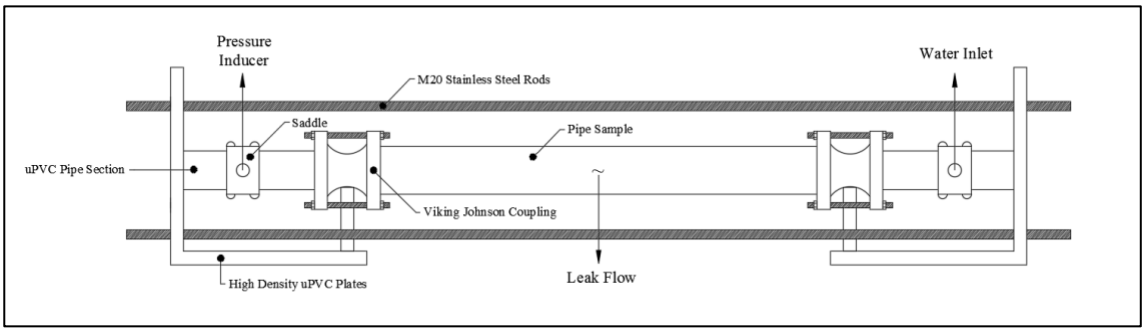

b)

Figure 1 | Schematic layout and photograph of the main components of the experimental setup.

The system was held together with three 20 mm diameter stainless steel rods secured to the end sections. The steel rods took up the longitudinal forces exerted by the water pressure and thus prevented longitudinal stresses being induced in the sample pipe walls. Test sections were all 800 mm long, leaving a minimum distance of 350 mm between the leak opening and pipe section end.

One end section was connected to a pumped water supply from an underground sump through a 25 mm calibrated magnetic flow meter with an accuracy of ±0.5%. The downstream end was fitted with a calibrated pressure transducer with a working range of 0–20 bar and accuracy of ±0.5%. Water was supplied by a variable speed submersible centrifugal pump capable of supplying a flow of 5 L/s at a head of 100 m.

At the start of an experimental run, a small flow was introduced and the setup tilted towards an opening on the downstream end to remove all trapped air. The setup was then placed horizontally with the pressure transducer and leak on the same level. The leak discharged into the atmosphere and no flow existed in the system apart from the leakage.

Flow and pressure were increased and then decreased in about five steps by varying the pump speed. Each step lasted about 30 seconds and was long enough to ensure that both flow and pressure readings stabilised. This procedure was repeated three times in succession before downloading and analysing the logged data. Data was collected at 1 second intervals and

generally consisted of between 900 and 1000 readings of pressure and flow rate. A typical raw data set is showed in Figure 2.

Experimental data points were obtained by identifying stable sections of the flow and pressure graphs and then taking the average values over each of the ranges. These (typically 25) average values were then plotted and analysed to determine the leakage characteristics for each experiment.

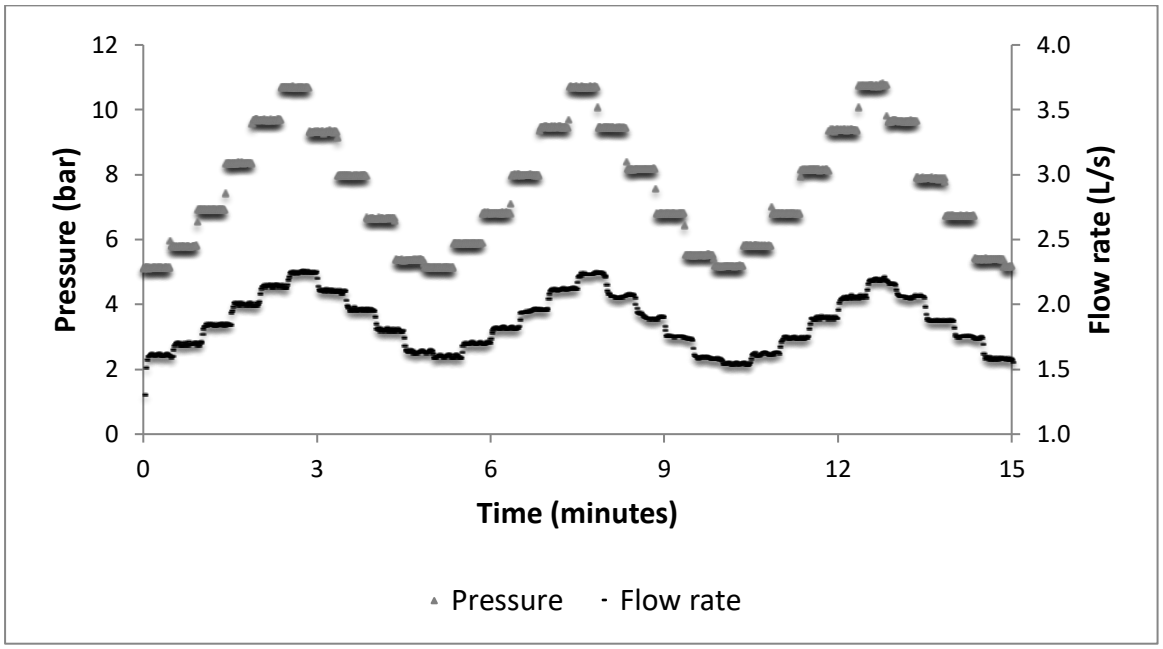

Figure 2 | Logged flow and pressure data for a typical experimental run.

It was observed that the first raising leg of tests on cracks in plastic pipes were often distinctly different from the rest of the data, possibly due to initial plastic deformation before the leak opening stabilised. In such cases the first few (between one and six) data points were omitted from the results.

RESULTS

The results of the experiments are summarized in Table 2. The analyses conducted to obtain these results are first explained, followed by a discussion of significant observations and their implications for leakage modelling.

Table 2 | Summary of experimental results

Pipe material	Length/ diameter (mm)	N1	A_0' (mm^2)	95% SCI* for A_0' (mm)	m' (mm^2/m)	95% SCI* for m' (mm^2/m)	p for m' (%)	C_d
Round holes								
uPVC	12	0.499	68.3	±0.11	-0.00141	±0.00230	12.5	0.603
mPVC	12	0.500	68.3	±0.17	0.00021	±0.00360	87.9	0.604
HDPE	12	0.501	70.3	±0.16	0.00180	±0.00345	4.5	0.621
Steel	12	0.497	67.4	±0.18	-0.00486	±0.00365	0.2	0.596
Longitudinal slits (width = 1 mm)								
uPVC	50	0.886	27.4	±2.08	0.28658	±0.0193	<0.1	0.547
uPVC	100	1.041	52.9	±2.59	2.51200	±0.129	<0.1	0.529
mPVC	50	0.989	37.5	±6.00	0.86711	±0.139	<0.1	0.749
HDPE	73	0.835	62.8	±11.7	0.97499	±0.348	<0.1	0.860
HDPE	100	0.798	94.5	±12.0	2.03031	±0.578	<0.1	0.945
Steel	50	0.500	22.0	±0.22	0.00011	±0.00275	10.3	0.440
Steel	100	0.529	44.7	±0.13	0.02166	±0.00205	<0.1	0.447
Spiral slits (width = 1 mm)								
uPVC	50	0.657	36.6	±0.53	0.10802	±0.00800	<0.1	0.732
uPVC	100	0.797	78.4	±1.31	1.24352	±0.0476	<0.1	0.784
mPVC	50	0.798	43.2	±1.47	0.37375	±0.0288	<0.1	0.865
HDPE	50	0.656	33.0	±3.08	0.09377	±0.0451	<0.1	0.660
HDPE	78	0.703	69.0	±4.68	0.48148	±0.123	<0.1	0.884
Steel	50	0.490	22.8	±0.08	–0.00267	±0.00095	6.4	0.457
Steel	105	0.523	44.2	±0.17	0.01615	±0.00265	1.6	0.421
Circumferential slits (width = 1 mm)								
uPVC	50	0.455	34.8	±0.26	–0.02170	±0.00380	<0.1	0.696
uPVC	100	0.327	50.2	±1.28	–0.11423	±0.0189	<0.1	0.502
mPVC	50	0.433	37.2	±0.27	–0.03403	±0.00380	<0.1	0.743
HDPE	54	0.185	20.6	±1.74	–0.06212	±0.0213	<0.1	0.382
HDPE	80	–0.262	37.4	±5.14	–0.20706	±0.0646	<0.1	0.467
Steel	53	0.499	22.6	±0.37	–0.00008	±0.00485	33.3	0.427

Note: * SCI = simultaneous confidence interval.

The leakage exponent *N1* (column 3 in Table 2) for each experiment was obtained by fitting a power curve to the flow against head data as shown for round holes in Figure 3.

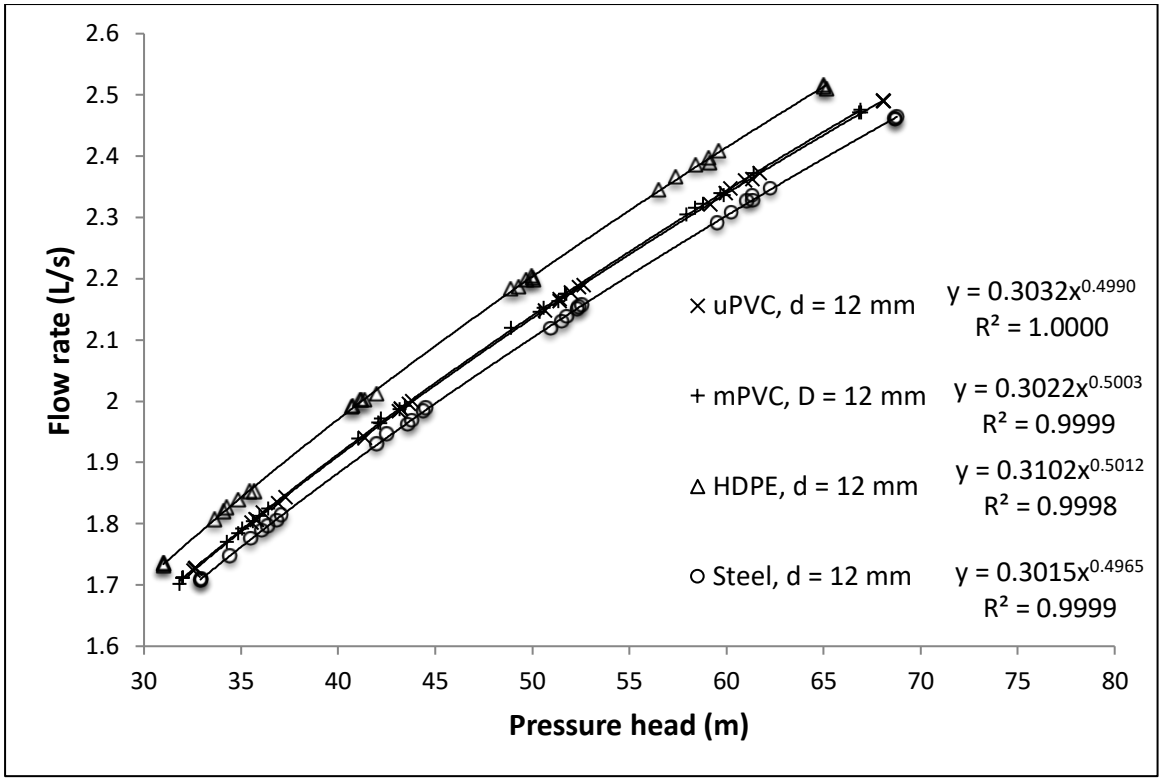

Figure 3 | Flow rate against pressure head for 12 mm diameter round holes in different pipe materials.

The effective leak area at each pressure was then calculated from Equation (1) and plotted against the pressure head as shown for longitudinal slits in Figure 4.

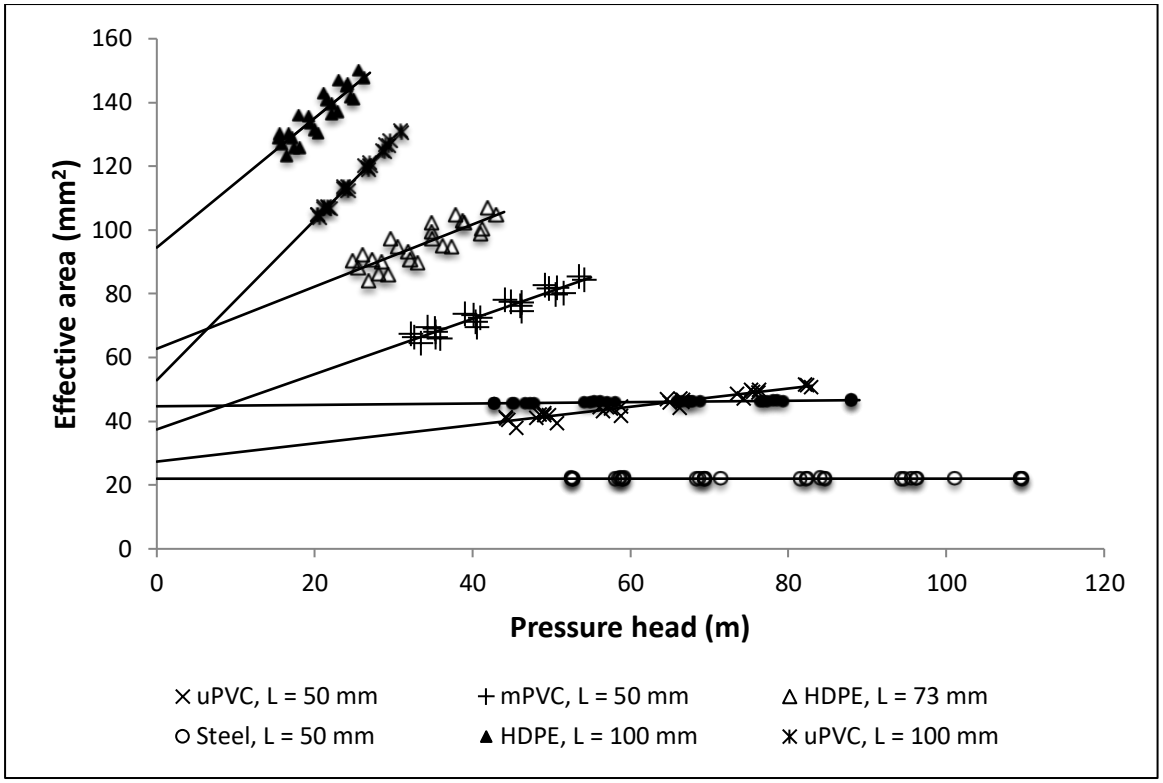

Figure 4 | Effective leak area against pressure head for longitudinal slits.

A linear model was fitted to the data points for each experiment to determine the model parameters and the 95% simultaneous confidence intervals for each parameter.

The statistical inference theory used to obtain the confidence intervals can be obtained from standard statistics text books such as Johnson & Wichern (2007). The model specifies a linear relationship of the form (compare to Equation (6)):

$$A_i' = A_0' + m_i' h_i + \varepsilon_i$$

where h_i and A_i' are the pressure head and effective area respectively for observation i (i=1,2,…,n), and ε_i, which captures noise, follows a normal distribution with a mean of zero and variance σ^2, and is independently drawn for each observation.

The intercept and slope of the linear relationship, contained in $\underline{\beta} = [A_0' \; m']'$, are estimated as $\underline{\hat{\beta}} = [\, \hat{A}_0' \; \hat{m}']'$ so as to maximise the likelihood function.

Assuming that one model parameter is known, the standard confidence interval limits for the other model parameter are given by:

$$\hat{\beta}_i \pm \; t_{n-2,0.025} s \sqrt{(X'X)_{ii}^{-1}}$$

where $t_{n-2,0.025}$ is the upper 2.5th percentile of a t-distribution with $n-2$ degrees of freedom.

However, since neither parameter can be assumed known in many cases, a more realistic estimate is obtained by considering the uncertainties in the two parameter values simultaneously, resulting in a two-dimensional 95% confidence region. This region for the simultaneous confidence limits for $\underline{\beta}$ may be determined using the equation:

$$\left\{\underline{\beta}\middle|\left(\underline{\hat{\beta}}-\underline{\beta}\right)'(X'X)\left(\underline{\hat{\beta}}-\underline{\beta}\right)\leq 2s^2F_{2,n-2,0.05}\right\}$$

where $F_{2,n-2,0.05}$ is the upper 5th percentile of an F-distribution with 2 and n-2 degrees of freedom; X is the n-by-2 design matrix (first column contains 1s, second column contains the h_i values); and s^2 is the estimated value of σ^2, and equals the sum of squared residuals (differences between observed A_i' values and fitted expected values) divided by n–2.

The simultaneous confidence interval widths for the experiments were found to be on average 27% (varying between 24.6 and 29.3%) larger than the single parameter confidence intervals.

The effective initial area and its 95% simultaneous confidence interval are given in columns 4 and 5 of Table 2 respectively. Similarly, the effective head-area slope and its 95% simultaneous confidence interval are given in columns 6 and 7.

The p-value in column 8 of Table 2 is the probability of observing the effective head-area slope or a more extreme estimate, where the true value of the head-area slope is equal to zero (null hypothesis: $m_i' = 0$). A small p-value provides evidence against this null.

The final column of Table 2 gives an estimate of the discharge coefficient of the leak openings. Since the initial area of the leak openings can be estimated from the pipe samples, it is possible to estimate the discharge coefficient by dividing the effective initial area by the actual initial area.

DISCUSSION

The results in Table 2 and Figure 1 show that the areas of 12 mm round holes varied very little with pressure for all pipe materials tested. Even at the largest absolute 95% interval, the effective head-area slopes were all below 0.01 mm^2/m. All the measured leakage exponent values were equal to the theoretical value of 0.50 at two significant digits.

This means that in practice 12 mm round holes (and likely a wider range of diameters) can be assumed fixed and thus to adhere to the orifice equation. For experimental studies, 12 mm round holes can be used as a benchmark for the accuracy and consistency of the results.

Steel pipes also displayed small head-area slopes with leakage exponents at or close to 0.50 for the range of leaks tested. Longer longitudinal and spiral slits displayed larger head-area slopes than shorter slit lengths (the same trend was observed for other pipe materials tested). These results support the practice of assuming N1 values of 0.5 for networks with steel or cast iron pipes. However, it should be noted that pipes with extensive corrosion damage may have larger N1 values as shown in a limited study using very low pressures by Greyvenstein (2007).

All circumferential slits tested were found to display negative head-area slopes, meaning that the areas of these slits decreased with increasing pressure resulting in leakage exponents below 0.5. Longer slits displayed more negative head-area slopes than shorter slits. The 80 mm long circumferential slit in HDPE had the most negative head-area slope and a negative N1 value, which means that not only the slit area, but also the flow rate through the slit decreased with increasing pressure.

The head-area slopes of longitudinal slits were found to be the largest of all the leak types tested, followed by spiral slits, particularly for longer slit lengths. Equation (4) was used to predict the head-area slopes for the longitudinal slits tested based on the values in Table 1 and assuming a discharge coefficient of 0.6 (Fox *et al.* 2016a) to calculate the effective head-area slope. The predicted effective head-area slopes are compared with the experimental values in Figure 5 showing good performance of the equation except for the 50 mm slit in a steel pipe, which for practical purposes had a fixed leak opening.

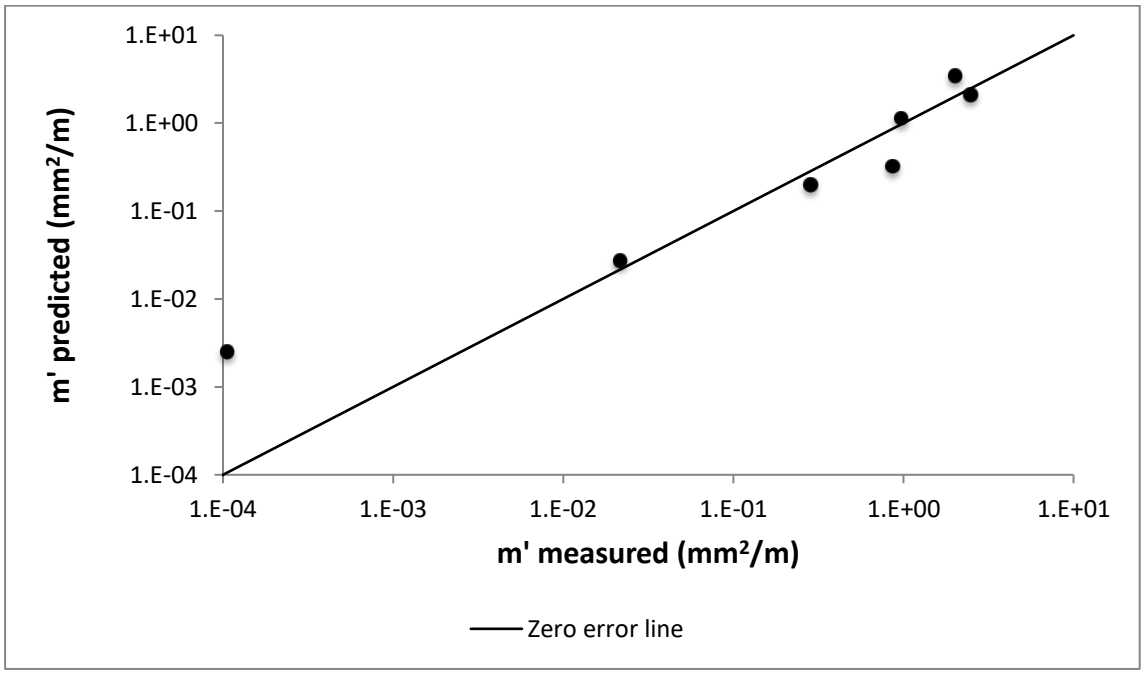

Figure 5 | Comparison of the effective head area slope predicted using Equation (4) and a discharge coefficient of 0.6 with the experimentally determined values.

It has been shown that the leakage exponents of most leaks are not fixed, but vary with fluid pressure (Van Zyl & Cassa 2014). While the experimental study only estimates a single overall N1 for each experiment, it is possible to calculate the actual range of N1 values for each experiment from the effective initial area, head area slope and the range of experimental test pressures. This is done by first calculating the leakage number for each data point using Equation (8) and then the leakage exponent at this pressure using Equation (9).

The range of leakage exponent values thus determined for each experiment is shown against the single value obtained by fitting a power equation to the data in Figure 6. The figure shows significant variation in the actual leakage exponent, except at the value of 0.5 where both methods give only theoretical value. The 80 mm circumferential slit in an HDPE pipe has a

particularly large leakage exponent range, which can be explained by its leakage number range (–0.28 to –0.63) starting to approach the asymptote at minus one in Equation (9).

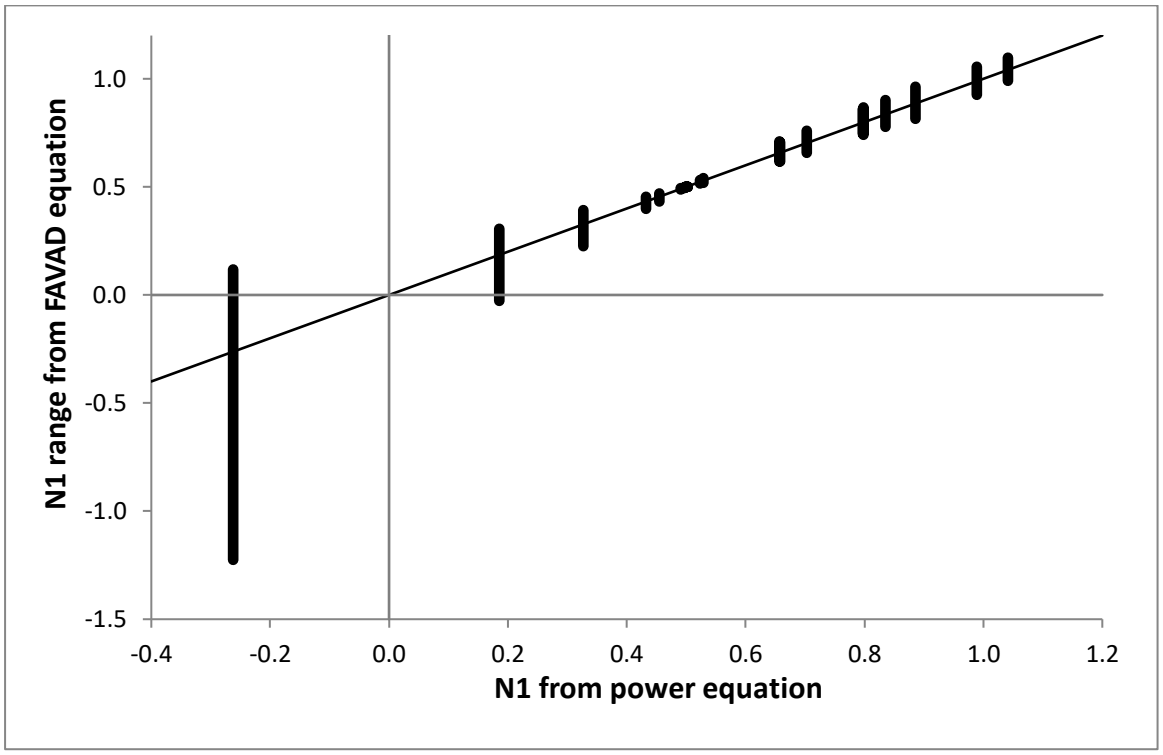

Figure 6 | The range of N1 values for each experiment against the single N1 determined experimentally.

Finally, the flow predictions of the N1 power and FAVAD equations are compared for 100 mm longitudinal slits in uPVC, HDPE and steel for a pressure range of zero to 100 m in Figure 7. The figure shows that both models fit the data well, but that there are large differences between the two equations for the uPVC and HDPE pipes outside the measured pressure range.

The FAVAD equation is based on a fundamental fluid mechanics theory, incorporating the linear head-area slope demonstrated in Figure 4. Thus it can be assumed to describe the true behaviour, while the empirical N1 equation results in significant modelling errors outside the measured pressure range. The capacity of the pumping system used in the experiment did not allow data to be collected at higher pressures, and thus further work is required to verify this assumption.

Both equations performed well on the steel pipe due to the practically zero head-area slope, and thus pure orifice flow that is equally well described with the FAVAD and N1 power equations.

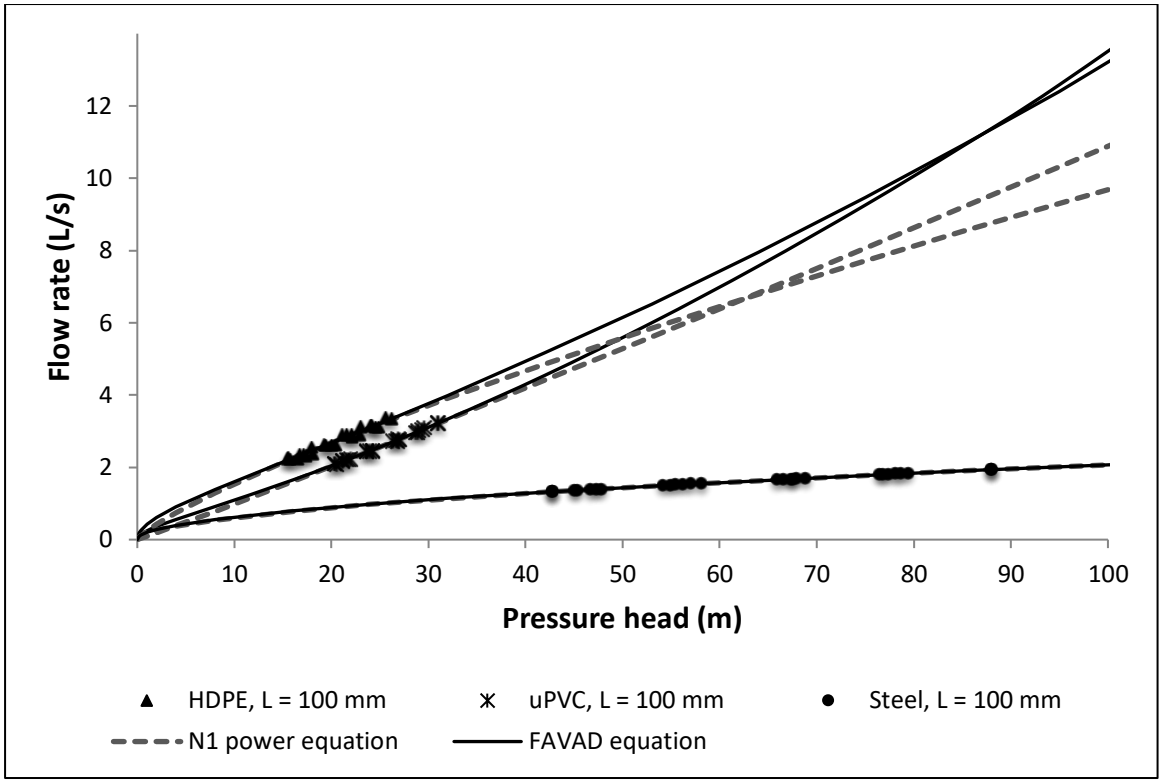

Figure 7 | Comparison of the N1 power and FAVAD equation flow predictions for 100 mm slits in uPVC, HDPE and steel pipes.

CONCLUSIONS

The aims of this paper were to provide a review of the developments in understanding the behaviour of leaks over the last decade and use these to interpret the results of a recent experimental study on the pressure-leakage behaviour of various leak types in different pipe materials.

Recent research has established that the areas of all leaks types vary as linear functions of pressure under both elastic and viscoelastic conditions. This behaviour can be characterised by determining the initial area and head-area slope of a leak opening.

It has been established and confirmed by this study that round holes have very small head-area slopes that can normally be assumed as zero, circumferential slits have small head-area slopes that are often negative and longitudinal slits have the largest head-area slopes. An equation for predicting the head-area slope of longitudinal slits (Cassa & Van Zyl 2013) was shown to perform reasonably well in this study.

Finally, the study showed that the N1 power equation produces good results when used within its calibrated range, but can result in significant errors when used outside this range.

ACKNOWLEDGEMENTS

The authors would like to acknowledgement the assistance of Reshma Kassanjee of the Statistical Consulting Service at the Department of Statistical Sciences, University of Cape Town for the statistical analysis, as well as Allan Lambert for constructive comments on the manuscript.

REFERENCES

Al-Ghamdi, A. S. 2011 Leakage-pressure relationship and leakage detection in intermittent water distribution systems. *J. Water Supply Res. Technol. AQUA* **60**(3), 178–183.

Buckley, R. S. 2007 *Theoretical investigation and experimentation into the expansion of round holes and cracks within pressurised pipes*. M.Eng. dissertation, Department of Civil Engineering, University of Johannesburg.

Cassa, A. M. & Van Zyl, J. E. 2013 Predicting the pressure-leakage slope of cracks in pipes subject to elastic deformations. *J. Water Supply Res. Technol. AQUA* **62**(4), 214–223.

Cassa, A. M., Van Zyl, J. E. & Laubscher, R. F. 2010 A numerical investigation into the effect of pressure on holes and cracks in water supply pipes. *Urban Water J.* **7**(2) 109–120.

De Marchis, M., Fontanazza, C. M., Freni, G., Notaro, V. & Puleo, V. 2016 Experimental evidence of leaks in elastic pipes. *Water Resour. Manage.* **30**, 2005–2019.

DPI 2010 *Design Guidelines for PVC Pressure Pipe Systems for Trenched Civil Applications.* DPI Plastics. Available from: www.dpiplastics.co.za/Documents/PVC%20Pipeline%20Design%20Guidelines%20Manual.pdf. Last accessed: 8 December 2016.

Farley, M. & Trow, S. 2003 *Losses in Water Distribution Network.* IWA Publishing, London.

Ferrante, M. 2012 Experimental investigation of the effects of pipe material on the leak head-discharge relationship. *J. Hydr. Eng. ASCE* **138**(8), 736–743.

Ferrante, M., Massari, C., Brunone, B. & Meniconi, S. 2011 Experimental evidence of hysteresis in the head-discharge relationship for a leak in a polyethylene pipe. *J. Hydr. Eng.* **137**(7), 775–780.

Ferrante, M., Meniconi, S. & Brunone, B. 2014 Local and global leak laws. *Water Resour. Manage.* 28(11), 3761–3782.

Ferrante, M., Massari, C., Brunone, B. & Meniconi, S. 2013 Leak behaviour in pressurized PVC pipes. *Water Sci. Technol. Water Supply* **13**(4), 987, 987-992.

Ferrante, M., Todini, E., Massari, C., Brunone, B. & Meniconi, S. 2013 Experimental investigation of leak hydraulics. *J. Hydroinform*. **15**(3), 666–675.

Fox, S., Collins, R. & Boxall, J. 2016a Experimental study exploring the interaction of structural and leakage dynamics. *J. Hydr. Eng*. **143**(2).

Fox, S., Collins, R. & Boxall, J. 2016b Physical investigation into the significance of ground conditions on dynamic leakage behaviour. *J. Water Supply Res. Technol. AQUA* **65**(2), 103–115.

Franchini, M. & Lanza, L. 2014 Leakages in pipes: generalizing Torricelli's equation to deal with different elastic materials, diameters and orifice shape and dimensions. *Urban Water J.* **11**(8), 678–695.

Gebhardt, D. S. 1975 The effects of pressure on domestic water supply including observations on the effect of limited water-gardening restrictions during a period of high demand. *WaterSA* 1(1), 3–8.

Greyvenstein, B. & van Zyl, J. E. 2007 An experimental investigation into the pressure-leakage relationship of some failed water pipes. *J. Water Supply Res. Technol. AQUA* **56**(2), 117-124.

Hiki, S. 1981 Relationship between leakage and pressure. *Jpn. Waterworks Assoc. J.* **May**, 50–54.

Idelchick, I. 1994 *Handbook of Hydraulic Resistance.* Begell House, Redding, CT.

Johnson, R. A. & Wichern, D. W. 2007 *Applied Multivariate Statistical Analysis*, 6th edn. Pearson, New York, 800 pp.

Kabaasha, A. M., Van Zyl, J. E. & Piller, O. 2016 Modelling pressure – leakage response in water distribution systems considering leak area variation. *14th International Conference on Computing and Control for the Water Industry*, CCWI2106, 7–9 November, Amsterdam, the Netherlands.

Lambert A. 1997 *Pressure Management: Leakage Relationships. Theory, Concepts and Practical Application.* Paper presented at IQPC Seminar, London.

Lambert A. 2000 What do we know about pressure: leakage relationship in distribution system? In: *System Approach to Leakage Control and Water Distribution Systems Management*. Brno, Czech Republic.

Lambert, A. 2015 *Water Leakage and Pressure Management: Welcome.* Available from: www.leakssuite.com. Last accessed: 15 December 2016.

Lambert, A. 2016 *Personal communication*.

Lambert, A., Fantozzi, M. & Thornton, J. 2013 Practical approaches to modeling leakage and pressure management in distribution systems – Progress since 2005. *International Conference on Computing and Control for the Water Industry*, CCWI2005, Exeter, UK. Available from: www.leakssuite.com/wp-content/uploads/2012/11/CCWI_Sep2013 paper_Pressure-burstsALMFJT-1-2003-2013K1.pdf

Ledochowski, W. 1956 An analytic method of locating leaks in pressure pipe-lines. *J. S. Afr. Inst. Civil Eng*. **6**(12) 341–344.

Massari, C., Ferrante, M., Brunone, B. & Meniconi, S. 2012 Is the leak head-discharge relationship in polyethylene pipes a bijective function? *J. Hydr. Res*. **50**, 409–417.

May, J. H 1994 *Pressure Dependent Leakage*. World Water and Environmental Engineering, October 1994. Available from: www.leakssuite.com/wp-content/uploads/2016/10/JOHN-MAY-SEMINAL-1994-ARTICLE-4.pdf.

May, J. H. 1994 Leakage, pressure and control. In: *Proceedings of the BICS International Conference Leakage Control Investing In Underground Assets*. The SAS Portman Hotel, London.

Ogura, L. 1979 Experiment on the relationship between leakage and pressure. *Jpn Water Works Assoc.* **June**, 38–45

Schwaller, J. & Van Zyl, J. E. 2014 Modeling the pressure-leakage response of water distribution systems based on individual leak behavior. *J. Hydr. Eng*. **141**(2)

Schwaller, J., Van Zyl, J. E. & Kabaasha, A. M. 2015 Characterising the pressure-leakage response of pipe networks using the FAVAD equation. *Water Sci. Technol. Water Supply* **15**(6), 1373–1382

Ssozi, E. N., Reddy, B. D. & Van Zyl, J. E. 2016 Numerical investigation of the influence of viscoelastic deformation on the pressure-leakage behavior of plastic pipes. *J. Hydr. Eng.* **142**(3).

Van Zyl, J. E. & Cassa, A. M. 2014 Modeling elastically deforming leaks in water distribution pipes. *J. Hydr. Eng.* **140**(2), 182–189.

Van Zyl, J. E. & Clayton, C. R. I. 2007 The effect of pressure on leakage in water distribution systems. *Water Manage.* **160**(WM2), 109–114.

Van Zyl, J. E., Lambert, A. O. & Collins, R. (in press) Realistic modeling of leakage and intrusion flows through leak openings in pipes. *J. Hydr. Eng.*

Walski, T., Bazts, W., Posluszny, E. T., Weir, M. & Whitman, B. E. 2006 Modeling leakage reduction through pressure control. *J. Am. Water Works Assoc*. 98(4)147–155.

First received 18 December 2016; accepted in revised form 19 April 2017. Available online